CLEO CONF 98-14
ICHEP98 869

Resonance structure of $\tau \to K^-\pi^+\pi^-\nu_\tau$ decays

CLEO Collaboration

(July 21, 1998)

Abstract

Using a sample of 4.7 fb^{-1} integrated luminosity accumulated with the CLEOII detector at the Cornell Electron Storage Ring (CESR), we investigate the mass spectrum and resonant structure in $\tau^- \to K^-\pi^+\pi^-\nu_\tau$ decays. Relative fractions of $K_1(1270)$ and $K_1(1400)$ resonances in these decays are measured. We study interference effects and the possibility of a non-zero strong phase in this process.

A. Anastassov,[1] J. E. Duboscq,[1] K. K. Gan,[1] T. Hart,[1] K. Honscheid,[1] H. Kagan,[1]
R. Kass,[1] J. Lee,[1] H. Schwarthoff,[1] A. Wolf,[1] M. M. Zoeller,[1] S. J. Richichi,[2] H. Severini,[2]
P. Skubic,[2] A. Undrus,[2] M. Bishai,[3] S. Chen,[3] J. Fast,[3] J. W. Hinson,[3] N. Menon,[3]
D. H. Miller,[3] E. I. Shibata,[3] I. P. J. Shipsey,[3] S. Glenn,[4] Y. Kwon,[4,*] A.L. Lyon,[4]
S. Roberts,[4] E. H. Thorndike,[4] C. P. Jessop,[5] K. Lingel,[5] H. Marsiske,[5] M. L. Perl,[5]
V. Savinov,[5] D. Ugolini,[5] X. Zhou,[5] T. E. Coan,[6] V. Fadeyev,[6] I. Korolkov,[6] Y. Maravin,[6]
I. Narsky,[6] R. Stroynowski,[6] J. Ye,[6] T. Wlodek,[6] M. Artuso,[7] E. Dambasuren,[7] S. Kopp,[7]
G. C. Moneti,[7] R. Mountain,[7] S. Schuh,[7] T. Skwarnicki,[7] S. Stone,[7] A. Titov,[7]
G. Viehhauser,[7] J.C. Wang,[7] J. Bartelt,[8] S. E. Csorna,[8] K. W. McLean,[8] S. Marka,[8] Z. Xu,[8]
R. Godang,[9] K. Kinoshita,[9] I. C. Lai,[9] P. Pomianowski,[9] S. Schrenk,[9] G. Bonvicini,[10]
D. Cinabro,[10] R. Greene,[10] L. P. Perera,[10] G. J. Zhou,[10] S. Chan,[11] G. Eigen,[11] E. Lipeles,[11]
J. S. Miller,[11] M. Schmidtler,[11] A. Shapiro,[11] W. M. Sun,[11] J. Urheim,[11] A. J. Weinstein,[11]
F. Würthwein,[11] D. E. Jaffe,[12] G. Masek,[12] H. P. Paar,[12] E. M. Potter,[12] S. Prell,[12]
V. Sharma,[12] D. M. Asner,[13] J. Gronberg,[13] T. S. Hill,[13] D. J. Lange,[13] R. J. Morrison,[13]
H. N. Nelson,[13] T. K. Nelson,[13] D. Roberts,[13] B. H. Behrens,[14] W. T. Ford,[14] A. Gritsan,[14]
H. Krieg,[14] J. Roy,[14] J. G. Smith,[14] J. P. Alexander,[15] R. Baker,[15] C. Bebek,[15]
B. E. Berger,[15] K. Berkelman,[15] V. Boisvert,[15] D. G. Cassel,[15] D. S. Crowcroft,[15]
M. Dickson,[15] S. von Dombrowski,[15] P. S. Drell,[15] K. M. Ecklund,[15] R. Ehrlich,[15]
A. D. Foland,[15] P. Gaidarev,[15] R. S. Galik,[15] L. Gibbons,[15] B. Gittelman,[15] S. W. Gray,[15]
D. L. Hartill,[15] B. K. Heltsley,[15] P. I. Hopman,[15] J. Kandaswamy,[15] D. L. Kreinick,[15]
T. Lee,[15] Y. Liu,[15] N. B. Mistry,[15] C. R. Ng,[15] E. Nordberg,[15] M. Ogg,[15,†] J. R. Patterson,[15]
D. Peterson,[15] D. Riley,[15] A. Soffer,[15] B. Valant-Spaight,[15] A. Warburton,[15] C. Ward,[15]
M. Athanas,[16] P. Avery,[16] C. D. Jones,[16] M. Lohner,[16] C. Prescott,[16] A. I. Rubiera,[16]
J. Yelton,[16] J. Zheng,[16] G. Brandenburg,[17] R. A. Briere,[17] A. Ershov,[17] Y. S. Gao,[17]
D. Y.-J. Kim,[17] R. Wilson,[17] H. Yamamoto,[17] T. E. Browder,[18] Y. Li,[18] J. L. Rodriguez,[18]
S. K. Sahu,[18] T. Bergfeld,[19] B. I. Eisenstein,[19] J. Ernst,[19] G. E. Gladding,[19] G. D. Gollin,[19]
R. M. Hans,[19] E. Johnson,[19] I. Karliner,[19] M. A. Marsh,[19] M. Palmer,[19] M. Selen,[19]
J. J. Thaler,[19] K. W. Edwards,[20] A. Bellerive,[21] R. Janicek,[21] P. M. Patel,[21] A. J. Sadoff,[22]
R. Ammar,[23] P. Baringer,[23] A. Bean,[23] D. Besson,[23] D. Coppage,[23] C. Darling,[23]
R. Davis,[23] S. Kotov,[23] I. Kravchenko,[23] N. Kwak,[23] L. Zhou,[23] S. Anderson,[24] Y. Kubota,[24]
S. J. Lee,[24] R. Mahapatra,[24] J. J. O'Neill,[24] R. Poling,[24] T. Riehle,[24] A. Smith,[24]
M. S. Alam,[25] S. B. Athar,[25] Z. Ling,[25] A. H. Mahmood,[25] S. Timm,[25] and F. Wappler[25]

[1]Ohio State University, Columbus, Ohio 43210
[2]University of Oklahoma, Norman, Oklahoma 73019
[3]Purdue University, West Lafayette, Indiana 47907
[4]University of Rochester, Rochester, New York 14627
[5]Stanford Linear Accelerator Center, Stanford University, Stanford, California 94309
[6]Southern Methodist University, Dallas, Texas 75275
[7]Syracuse University, Syracuse, New York 13244

[*]Permanent address: Yonsei University, Seoul 120-749, Korea.

[†]Permanent address: University of Texas, Austin TX 78712.

[8]Vanderbilt University, Nashville, Tennessee 37235
[9]Virginia Polytechnic Institute and State University, Blacksburg, Virginia 24061
[10]Wayne State University, Detroit, Michigan 48202
[11]California Institute of Technology, Pasadena, California 91125
[12]University of California, San Diego, La Jolla, California 92093
[13]University of California, Santa Barbara, California 93106
[14]University of Colorado, Boulder, Colorado 80309-0390
[15]Cornell University, Ithaca, New York 14853
[16]University of Florida, Gainesville, Florida 32611
[17]Harvard University, Cambridge, Massachusetts 02138
[18]University of Hawaii at Manoa, Honolulu, Hawaii 96822
[19]University of Illinois, Urbana-Champaign, Illinois 61801
[20]Carleton University, Ottawa, Ontario, Canada K1S 5B6
and the Institute of Particle Physics, Canada
[21]McGill University, Montréal, Québec, Canada H3A 2T8
and the Institute of Particle Physics, Canada
[22]Ithaca College, Ithaca, New York 14850
[23]University of Kansas, Lawrence, Kansas 66045
[24]University of Minnesota, Minneapolis, Minnesota 55455
[25]State University of New York at Albany, Albany, New York 12222

I. INTRODUCTION

Decays of the τ lepton into three pseudoscalars have been actively studied over the last several years. Lately, a number of relatively precise measurements of the branching fractions for $\tau^- \to K^-\pi^+\pi^-\nu_\tau$ have become available from ALEPH, CLEO and OPAL [1–4]. However, the resonance substructure of these decays has not yet been measured with high precision.

The decay $\tau^- \to K^-\pi^+\pi^-\nu_\tau$, with its simple and well-understood initial state provides information on low-Q^2 QCD. The effects of $SU(3)_f$ symmetry breaking can be observed in this decay, the decay constants of the K_1 resonances can be measured, and the hadronic resonance substructure can be studied from an analysis of the final state invariant mass spectra [5,6]. Other interesting topics include resonance parameters (such as the widths of the K_1 states), tests of isospin relations, measurements of the Wess-Zumino anomaly, etc. Current models of this decay [7,8] are based on Chiral Perturbation Theory (CHPT) calculations. Our measurements will help to test these models.

The primary goal of this analysis is to measure the relative amplitudes of the $K_1(1270)$ and $K_1(1400)$ resonances that are believed to dominate $\tau^- \to K^-\pi^+\pi^-\nu_\tau$ decays [7,8]. Based on the data, we suggest a parameterization of the form-factors describing the dynamics of this decay somewhat different from currently accepted models [9].

II. THEORETICAL ASPECTS OF $\tau^- \to K^-\pi^+\pi^-\nu_\tau$ DECAYS

In the Standard Model, the general form for the semileptonic τ-decay matrix element can be written as [9]:

$$\mathcal{M} = \frac{G}{\sqrt{2}}\bar{u}(p_\nu)\gamma^\mu(v + a\gamma_5)u(p_\tau)J_\mu \tag{1}$$

where $J_\mu \equiv \langle K\pi\pi|V_\mu - A_\mu|0\rangle$ is the hadronic current, and p_ν and p_τ are the four-momenta of the τ neutrino and the τ lepton, respectively

General considerations based on Lorenz invariance and conservation of energy and momentum lead to the conclusion that only four independent form-factors are needed to describe the hadronic current in $\tau^- \to K^-\pi^+\pi^-\nu_\tau$ [7,8]:

$$\begin{aligned} J_\mu = &(F_1(s_1, s_2, Q^2)(p_1 - p_3)_\nu + F_2(s_1, s_2, Q^2)(p_2 - p_3)_\nu)T^{\mu\nu} \\ &+ F_a(s_1, s_2, Q^2)\epsilon^{\mu\nu\rho\sigma}p_{1\nu}p_{2\rho}p_{3\sigma} + F_s(s_1, s_2, Q^2)Q^\mu, \end{aligned} \tag{2}$$

where F_i are form-factors, Q^μ is the 4-vector of $K\pi\pi$, $s_1 = (p_2 + p_3)^2$, $s_2 = (p_1 + p_3)^2$ and $T^{\mu\nu} = (g^{\mu\nu} - Q^\mu Q^\nu/Q^2)$. There are two axial vector form factors F_1 and F_2, an anomalous vector form factor F_a, and a scalar form-factor F_s.

To derive specific expressions for the form-factors, some assumptions have to be made. It is believed [7,8] that this decay is dominated by the lowest-mass resonances. There are two axial vector resonances which can produce the $K^-\pi^+\pi^-$ final state. These are the weak eigenstates $^3P_1$ and $^1P_1$ $(u\bar{s})$, called K_a and K_b. Of these, the K_b couples to the W as a "second class" current, violating $SU(3)_f$ symmetry. These two weak eigenstates mix to form the observable mass eigenstates, $K_1(1270)$ and $K_1(1400)$ [5]. The $K_1(1270)$ subsequently decays into $K^*\pi$ and $K\rho$ while the $K_1(1400)$ decays almost entirely to $K^*\pi$. With these intermediate states, the form-factors can be written as [8]:

$$F_1 = \frac{\sqrt{2}}{3} \cdot BW_{K_1(1270)} \frac{BW_\rho + \xi BW_{\rho'}}{1+\xi} \tag{3}$$

$$F_2 = -\frac{\sqrt{2}}{3} \cdot \frac{\eta BW_{K_1(1270)} + BW_{K_1(1400)}}{(1+\eta)} \cdot BW_{K^*}, \tag{4}$$

where BW denotes a Breit-Wigner mass distribution. The parameter η is estimated to be 0.33 in [8]. The coefficients preceding the Breit-Wigner expressions are fixed by Chiral Perturbation Theory. In the first form-factor, the coefficient ξ is determined to be -0.145 using Conservation of Vector Current (CVC) from $e^+e^- \to \pi^+\pi^-$ data [8,10].

In the chiral limit, the scalar form-factor F_s is zero. The vector form-factor F_a is numerically small compared to F_1 and F_2, and is only non-zero due to the Wess-Zumino anomaly. Its form is given by the following equation [9]:

$$F_a = -\sqrt{2} BW_{K^*} \frac{\epsilon BW_{K^*} + BW_\rho}{1+\epsilon}, \tag{5}$$

where $\epsilon = 0.2$.

A similar model is used in this analysis of the invariant mass distributions in $\tau^- \to K^-\pi^+\pi^-\nu_\tau$. However, our parameterization of the axial vector form-factors is somewhat different, as will be described later.

III. DATA SAMPLE AND EVENT SELECTION

Our data sample contains approximately 4.3 million τ-pairs produced in e^+e^- collisions, corresponding to an integrated luminosity of 4.7 fb^{-1}. The data were collected with the CLEOII detector [11] at the Cornell Electron Storage Ring, operating at a center-of-mass energy approximately 10.58 GeV.

The CLEO II detector is a general purpose solenoidal magnet spectrometer and calorimeter. The detector was designed for efficient triggering and reconstruction of two-photon, tau-pair, and hadronic events. Measurements of charged particle momenta are made with three nested coaxial drift chambers consisting of 6, 10, and 51 layers, respectively. These chambers fill the volume from r=3 cm to r=1 m, with r the radial coordinate relative to the beam ($\hat{z}$) axis. This system is very efficient ($\epsilon \geq$98%) for detecting tracks that have transverse momenta (p_T) relative to the beam axis greater than 200 MeV/c, and that are contained within the good fiducial volume of the drift chamber ($|\cos\theta| <$0.94, with θ defined as the polar angle relative to the beam axis). The charged particle detection efficiency in the fiducial volume decreases to approximately 90% at $p_T \sim$100 MeV/c. For $p_T <$100 MeV/c, the efficiency decreases roughly linearly to zero at a threshold of $p_T \approx$30 MeV/c. This system achieves a momentum resolution of $(\delta p/p)^2 = (0.0015p)^2 + (0.005)^2$ (p is the momentum, measured in GeV/c). Pulse-height measurements in the main drift chamber provide specific ionization (dE/dx) resolution of 5.5% for Bhabha events, giving good K/π separation for tracks with momenta up to 700 MeV/c and nearly 2σ separation in the relativistic rise region above 2 GeV/c. Outside the central tracking chambers are plastic scintillation counters, which are used as a fast element in the trigger system and also provide particle identification information from time-of-flight measurements.

Beyond the time-of-flight system is the electromagnetic calorimeter, consisting of 7800 thallium-doped CsI crystals. The central "barrel" region of the calorimeter covers about 75% of the solid angle and has an energy resolution which is empirically found to follow:

$$\frac{\sigma_{\rm E}}{E}(\%) = \frac{0.35}{E^{0.75}} + 1.9 - 0.1E; \tag{6}$$

E is the shower energy in GeV. This parameterization includes effects such as noise, and translates to an energy resolution of about 4% at 100 MeV and 1.2% at 5 GeV. Two end-cap regions of the crystal calorimeter extend solid angle coverage to about 95% of 4π, although energy resolution is not as good as that of the barrel region. The tracking system, time of flight counters, and calorimeter are all contained within a superconducting coil operated at 1.5 Tesla. Flux return and tracking chambers used for muon detection are located immediately outside the coil and in the two end-cap regions.

We select $e^+e^- \to \tau^+\tau^-$ events having a "1vs3" topology in which one τ lepton decays into one charged particle (plus possible neutrals), and the other τ lepton decays into 3 charged hadrons (plus possible neutrals). An event is separated into two hemispheres based on the measured event thrust axis.[1] Loose cuts on ionization measured in the drift chamber, energy deposited in the calorimeter and the maximum penetration depth into the muon detector system are applied to charged tracks in the signal (3-prong) hemisphere to reject leptons. Backgrounds from non-signal τ decays and hadronic events with K^0_S are suppressed by requirements on impact parameters of charged tracks. To reduce the background from two-photon collisions ($e^+e^- \to e^+e^-\gamma\gamma$ with $\gamma\gamma \to$hadrons or $\gamma\gamma \to l^+l^-$), cuts on visible energy (E_{vis}) and total event transverse momentum (P_t) are applied: 2.5 GeV $< E_{vis} <$ 10 GeV, and $P_t >$0.3 GeV/c. We also require the invariant mass of the tracks and showers in the 3-prong hemisphere, calculated under the $\pi^-\pi^+\pi^-$ hypothesis, to be less than 1.7 GeV/c.

Events are accepted for which the tag hemisphere (1-prong side) is consistent with one of the following four decays: $\tau^+ \to e^+\nu_e\overline{\nu}_\tau$, $\tau^+ \to \mu^+\nu_\mu\overline{\nu}_\tau$, $\tau^+ \to \pi^+\overline{\nu}_\tau$, or $\tau^+ \to \rho^+\overline{\nu}_\tau$.

Candidate events are distinguished from background τ decays with π^0's and continuum hadronic background ($e^+e^- \to q\bar{q}$) by the characteristics of showers in the electro-magnetic calorimeter. A photon candidate is defined as a shower in the barrel region of the electromagnetic calorimeter with energy above 40 MeV having an energy deposition pattern consistent with true photons. It must be separated from the closest charged track by at least 30 cm. $\tau^- \to K^-\pi^+\pi^-\nu_\tau$ candidates are defined as those events having zero photons with energy above 100 MeV in the 3-prong hemisphere.

The event selection described above provides a sample of events that contains $\tau^- \to \pi^-\pi^+\pi^-\nu_\tau$, $\tau^- \to K^-\pi^+\pi^-\nu_\tau$ and $\tau^- \to K^-K^+\pi^-\nu_\tau$. In this analysis we neglect possible

[1]The thrust axis of an event is chosen so that the sum of longitudinal (relative to this axis) momenta of all charged tracks has a maximum value.

contributions from the decays $\tau^- \to \pi^- K^+ \pi^- \nu_\tau$ and $\tau^- \to K^- \pi^+ K^- \nu_\tau$ because they are extremely small in the Standard Model and have not been experimentally observed. We also neglect the $\tau^- \to K^- K^+ K^- \nu_\tau$ final state. This rate is expected to be $\sim 1\%$ relative to that for $\tau^- \to K^- \pi^+ \pi^- \nu_\tau$ due to the limited phase space and the low probability of $(s\bar{s})$ popping.

IV. RECONSTRUCTION OF INVARIANT MASS SPECTRA

Due to the very small fraction of kaons in $\tau^- \to h^- h^+ h^- \nu_\tau$ events[2] and the limited particle ID capabilities of the CLEOII detector, it is difficult to identify individual $\tau^- \to K^- \pi^+ \pi^- \nu_\tau$ decays. In this analysis, a statistical approach is used in which the number of $\tau^- \to K^- h^+ \pi^- \nu_\tau$ events in any given sample is determined by analysis of dE/dx information of the two same-sign tracks in the signal hemisphere. The dE/dx analysis is described in detail in [12].

For each $h^- h^+ h^-$ candidate the invariant mass of the three hadrons is calculated under two hypotheses for the first and the third tracks, corresponding to $K^- \pi^+ \pi^-$ and $\pi^- \pi^+ K^-$. Each of these two sub-samples is divided into bins of invariant mass. The bins are 100 MeV/c^2 wide, spanning the region $0.8 - 1.7$ MeV/c^2. After binning in mass, the sub-samples that correspond to the same mass bin are combined.

The dE/dx analysis provides the number of kaons in each mass bin, which is equal to the number of $\tau^- \to K^- h^+ \pi^- \nu_\tau$ events in this mass interval. The invariant mass spectrum of the $K^- \pi^+ \pi^-$ system is thereby reconstructed. Obviously, this distribution contains a contribution from $\tau^- \to K^- K^+ \pi^- \nu_\tau$ decays, as will be discussed in Sec.V.

In a similar way the invariant mass spectra of $K^- \pi^+$ and $\pi^+ \pi^-$ are reconstructed in ten bins over the range 0.5 GeV/c^2 $< M_{K\pi} <$1.5 GeV/c^2 and 0.2 GeV/c^2 $< M_{\pi\pi} <$ 1.2 GeV/c^2, respectively. The reconstructed mass spectra are shown in Fig. 1.

V. BACKGROUND AND EFFICIENCY

There are two main types of background: continuum hadronic events ($e^+ e^- \to q\bar{q} \to$ *hadrons*) and non-signal τ decays. Hadronic background is estimated from a continuum hadronic Monte Carlo sample (using the JETSET v7.3 [13] event generator and GEANT [14] simulation code). This background is subtracted as described in [12]. The level of hadronic background is approximately 3%.

τ-related background comes primarily from $\tau^- \to K^- K^+ \pi^- \nu_\tau$ decays. These events comprise $\approx 27\%$ of the events in our reconstructed invariant mass distributions. Smaller components are $\tau^- \to K^- h^+ \pi^- \pi^0 \nu_\tau$ with incomplete π^0 reconstruction and decays to the $Kh\pi(\pi^0)$ final state involving K^0_S. These two backgrounds comprise 5% and 3% of the events in the $K^- \pi^+ \pi^-$ invariant mass spectra, respectively. The invariant mass distributions for backgrounds are found using Monte Carlo simulations to obtain the shape; the normalization is set by the measured branching fractions [12,15]. The background predictions are shown

[2]Here and later h designates either kaon or pion.

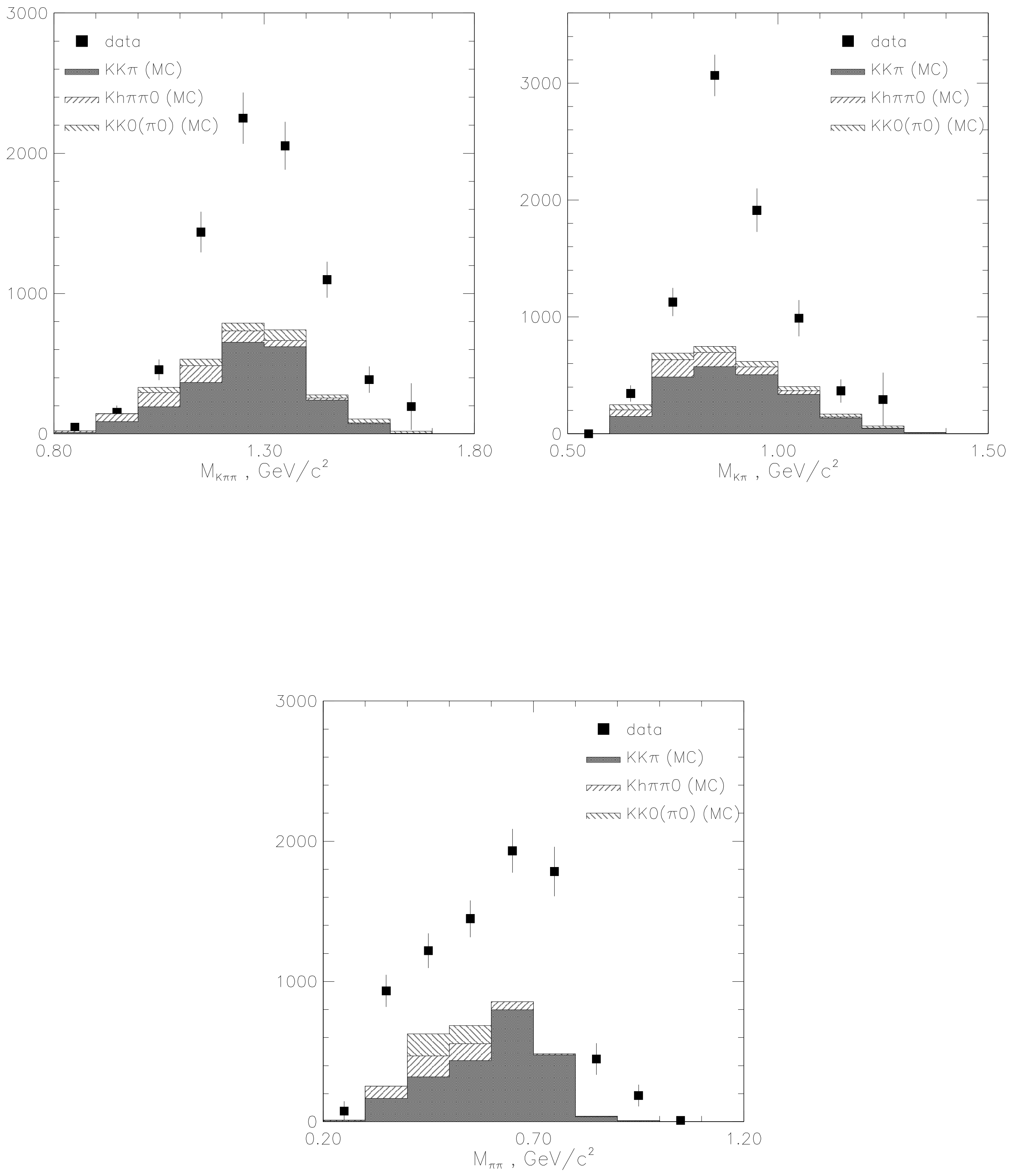

FIG. 1. Reconstructed mass spectra and predicted background.

in Fig. 1. The invariant mass distributions for all backgrounds are subtracted from the corresponding invariant mass spectra reconstructed from data.

The efficiency of event reconstruction depends slightly on the invariant mass. Therefore, it is necessary to introduce a mass-dependent efficiency correction. This correction is calculated from τ Monte Carlo using the KORALB event generator [9]. The maximum variation in efficiency across the mass interval of interest is of order 10%.

VI. FITTING METHOD

The hadronic structure of the $K^-\pi^+\pi^-$ system is investigated by simultaneously fitting three invariant mass distributions: $M_{K\pi\pi}$, $M_{K\pi}$ and $M_{\pi\pi}$. The fitting function is based upon a model similar to the one described in Sec. I, and now outlined in greater detail.

A. Parameterization of form-factors

Our main goal in this analysis is to determine the ratio of $\tau \to K_1(1270)\nu_\tau$ to $\tau \to K_1(1400)\nu_\tau$. Using the tabulated branching fractions of the K_1 resonances [15]:

$$\mathcal{B}(K_1(1270) \to K^*\pi) = (16 \pm 5)\% \tag{7}$$

$$\mathcal{B}(K_1(1270) \to K\rho) = (42 \pm 6)\% \tag{8}$$

$$\mathcal{B}(K_1(1400) \to K^*\pi) = (94 \pm 6)\% \tag{9}$$

$$\mathcal{B}(K_1(1400) \to K\rho) = (3 \pm 3)\% \tag{10}$$

and the isospin relations (see Appendix A) we obtain the following expression for the axial vector form-factors F_1 and F_2:

$$F_1 = \frac{1}{\sqrt{3}}((1-\alpha)\sqrt{0.42}BW_{1270} + \alpha\sqrt{0.03}BW_{1400})\frac{BW_\rho + \xi BW_{\rho'}}{1+\xi} \tag{11}$$

$$F_2 = -\frac{2}{3}((1-\alpha)\sqrt{0.16}BW_{1270} + \alpha\sqrt{0.94}BW_{1400})BW_{K^*} \quad , \tag{12}$$

where α defines the relative admixture of the K_1 resonances. The Breit-Wigner distributions for the K_1 resonances are defined following the approach of [9] as:

$$BW(s, m_{K_1}, \Gamma_{K_1}) = \frac{m_{K_1}^2 - i m_{K_1}\Gamma_{K_1}}{m_{K_1}^2 - s - i m_{K_1}\Gamma_{K_1}} \quad , \tag{13}$$

where the widths and masses of the K_1 resonances are set to world average values [15]:

$$M_{K_1(1270)} = 1273 MeV/c^2 \qquad \Gamma_{K_1(1270)} = 90 MeV/c^2$$

$$M_{K_1(1400)} = 1402 MeV/c^2 \qquad \Gamma_{K_1(1400)} = 174 MeV/c^2$$

The Breit-Wigner for the K^* and ρ resonances contains mass-dependent widths:

$$BW(s, m, \Gamma) = \frac{m^2}{m^2 - s - i\sqrt{s}\Gamma(s)}, \tag{14}$$

where the mass-dependence is defined by Eq. (22) in [9]. In Eqs. (13) and (14), the variable s is the three- and two-body invariant mass, respectively.

In this analysis, we have determined the numerical coefficients for the Breit-Wigner terms ($\sqrt{\frac{1}{3}}$ and $-\frac{2}{3}$) using isospin relations rather than taking the chiral limit as in [8]. The Wess-Zumino anomaly term is set to zero in our model because its amplitude relative to the axial vector form-factors is unknown. This term is numerically small enough that it can be neglected at our level of accuracy. (Appropriate systematic errors are assigned to reflect the possible magnitude of this contribution. One needs to keep in mind, however, that if the Wess-Zumino anomaly is much higher than expected, the $K^{*'}$ may contribute events to the region of $M_{K\pi\pi}$ invariant mass close to 1400 MeV/c^2, affecting our measurement of α.) Note also that we explicitly assume all $\tau^- \to K^-\pi^+\pi^-\nu_\tau$ decays proceed through either $K_1(1270)$ or $K_1(1400)$.

Since there may be a phase shift between the terms in the form-factors F_1 and F_2, we add three phases θ_1, θ_2 and θ_3 to describe possible interference effects. Phase differences may appear between various decay chains producing the final state $K^-\pi^+\pi^-$. This may cause additional constructive or destructive interference and, for example, enhance or suppress the ρ peak in the distribution of $\pi\pi$ invariant mass. In our model the three independent phase angles θ_1, θ_2 and θ_3 correspond to the following interfering decay chains:

$$\theta_1: \quad \tau \to K_1(1270)\nu_\tau \to K\rho\nu_\tau \to K\pi\pi\nu_\tau \quad and \quad \tau \to K_1(1400)\nu_\tau \to K\rho\nu_\tau \to K\pi\pi\nu_\tau \tag{15}$$

$$\theta_2: \quad \tau \to K_1(1270)\nu_\tau \to K^*\pi\nu_\tau \to K\pi\pi\nu_\tau \quad and \quad \tau \to K_1(1400)\nu_\tau \to K^*\pi\nu_\tau \to K\pi\pi\nu_\tau \tag{16}$$

$$\theta_3: \quad \tau \to K\rho\nu_\tau \to K\pi\pi\nu_\tau \quad and \quad \tau \to K^*\pi\nu_\tau \to K\pi\pi\nu_\tau \quad \text{via } K_1(1270) \text{ or } K_1(1400) \tag{17}$$

The form-factors then become:

$$F_1 = \frac{1}{\sqrt{3}}((1-\alpha)\sqrt{0.42}BW_{1270} + \alpha\sqrt{0.03}BW_{1400}e^{i\theta_1})\frac{BW_\rho + \xi BW_{\rho'}}{1+\xi}e^{i\theta_3} \tag{18}$$

$$F_2 = -\frac{2}{3}((1-\alpha)\sqrt{0.16}BW_{1270} + \alpha\sqrt{0.94}BW_{1400}e^{i\theta_2})BW_{K^*} \tag{19}$$

Studies of Monte Carlo samples have shown that at our level of statistics the sensitivity to the phase θ_1 is very low because the branching fraction of $K_1(1400)$ to $K\rho$ is only 3%. Therefore, in fitting data, this parameter is fixed to zero.

B. Fitting function

We use a Monte Carlo based fitting procedure, in which simulated events are used to fit the data distributions for $M_{K\pi\pi}$, $M_{K\pi}$ and $M_{\pi\pi}$. We determine the input parameters α, θ_2 and θ_3 which give the best match to data. In this way we can account for all interference effects between $K_1(1270)$ and $K_1(1400)$ as well as the $K^*\pi$ and $K\rho$ intermediate states.

As outlined above, our event generator is identical to KORALB [9] except that our form-factors (Eqs.(18)-(19)) are used and the Wess-Zumino form-factor is set to zero. To take into account finite resolution effects we introduce Gaussian smearing of the calculated mass equal to the smearing found from the full GEANT-based [14] simulation of the detector. This smearing is typically 5-10 MeV/c^2.

VII. ANALYSIS OF RESONANCE STRUCTURE

A. Determination of K_1 amplitudes

The most simple parameterization of the matrix element corresponds to the form-factors given in Eq.(11)-(12) and contains one free parameter α. In such a parameterization the dependence on the phases θ is ignored. The results of such a data fit are shown in Fig. 2. There is obvious disagreement in shape between the MC distribution and the data points. This disagreement persists when we switch to the parameterization of form-factors used in [9,8].

When the phase shifts are introduced as in Eq.(18)-(19), the fit improves substantially (Fig. 1). The best values for the fit parameters are now:

$$\alpha = 0.398 \pm 0.016 \pm 0.088$$

$$\theta_2 = (0.69 \pm 0.02 \pm 0.05) \cdot 2\pi$$

$$\theta_3 = (0.74 \pm 0.09 \pm 0.12) \cdot 2\pi,$$

where the first error is statistical and the second is systematic (described in detail later).

The ratio of amplitudes of the K_1 resonances is given by the following expression:

$$\frac{A(\tau \to K_1(1270)\nu)}{A(\tau \to K_1(1400)\nu)} \equiv \frac{1-\alpha}{\alpha} \times \Phi = (1.513 \pm 0.10 \pm 0.56) \times \Phi. \tag{20}$$

Φ depends on phase space and kinematical factors for $\tau^- \to K_1(1270)^-\nu_\tau$ relative to $\tau^- \to K_1(1400)^-\nu_\tau$. In principle, Φ also depends upon the masses and widths of the K_1 resonances. In the narrow width approximation, in which the masses of the two resonances are fixed at 1270 and 1400 MeV/c^2, respectively, $\Phi^2 \approx 1.8$ [5].

The value of α measured in this analysis can be compared to a similar parameter η used in the model [8] described in Sec. II. The relation between η (Eq.(3)-(4)) and α is:

$$\alpha = \frac{C_1}{\eta C_2 + C_1}, \tag{21}$$

where $C_1 = \mathcal{B}(K_1(1270) \to K^*\pi)$ and $C_2 = \mathcal{B}(K_1(1400) \to K^*\pi)$. Equation (21) is obtained by dividing the expression for F_2 given in Eq. (12) by $(1-\alpha)C_1 + \alpha C_2$ and comparing it to Eq. (4). (This is an approximate relation since the authors of [8] set the $K\rho$ component of $K_1(1400)$ to zero.) The value $\eta = 0.33$ used in [8] corresponds to $\alpha = 0.58$ which is somewhat different from our measurement.

From our result for the ratio of $\tau \to K_1\nu_\tau$ decay amplitudes, information about the mixing of the K_a and K_b eigenstates can be derived. The mixing between K_a and K_b is traditionally parameterized in the following way [5]:

$$K_1(1400) = K_a \cos\theta_K - K_b \sin\theta_K$$

$$K_1(1270) = K_a \sin\theta_K + K_b \cos\theta_K$$

In the case of exact $SU(3)_f$ symmetry, the second-class current $\tau \to K_b\nu_\tau$ is forbidden and only K_a is produced. However due to the difference between the masses of the up and strange quarks we may expect symmetry breaking effects of order $|\delta| = (m_s - m_u)/\sqrt{2}(m_s + m_u) \approx 0.18$. Then, instead of pure K_a a linear combination $|K_a\rangle - \delta|K_b\rangle$ is produced and the ratio of decay rates of the K_1 resonances can be written as [5]:

$$\frac{\mathcal{B}(\tau \to K_1(1270)\nu)}{\mathcal{B}(\tau \to K_1(1400)\nu)} = \left|\frac{\sin\theta_K - \delta\cos\theta_K}{\cos\theta_K + \delta\sin\theta_K}\right|^2 \times \Phi^2 \tag{22}$$

Squaring Eq. (20), and equating it to the right-hand side of Eq. (22), one can calculate θ_K:

$$\theta_K = \arctan\frac{1-\alpha(1-\delta)}{\alpha(1+\delta)-\delta} \tag{23}$$

There are two possible solutions, depending upon the sign of δ:

$$\begin{array}{l} \text{(a) } \theta_K = (67 \pm 10)^\circ \text{ for } \delta = 0.18, \\ \text{(b) } \theta_K = (46 \pm 10)^\circ \text{ for } \delta = -0.18. \end{array}$$

The quoted errors reflect statistical and experimental systematic errors, we have not yet fully assessed possible theoretical systematic errors.

One can also calculate θ_K using the current experimental information on the masses and branching fractions of $K_1(1270)$ and $K_1(1400)$ independent of their production in τ-decays. There are two possible solutions, $\theta_K \approx 33^\circ$ and $\theta_K \approx 57^\circ$ [5]. Our result has the same two-fold ambiguity and agrees well with this calculation.

The ratio of branching fractions for $\tau \to K_1\nu_\tau$ can be calculated from Eq. (20), and independent of θ_K, as the ratio of amplitudes squared:

$$\frac{\mathcal{B}(\tau \to K_1(1270)\nu)}{\mathcal{B}(\tau \to K_1(1400)\nu)} = 4.1 \pm 0.5 \pm 3.0 \tag{24}$$

One of the first measurements of the $\tau \to K_1\nu_\tau$ branching fractions was performed by the $TPC/2\gamma$ collaboration in 1994 [16]. Their results are $\mathcal{B}(\tau \to K_1(1270)\nu) = 0.41^{+0.41}_{-0.35}\%$ and $\mathcal{B}(\tau \to K_1(1400)\nu) = 0.76^{+0.40}_{-0.33}\%$, giving the ratio (24) to be $0.54^{+0.61}_{-0.52}$. The results of the $TPC/2\gamma$ experiment suggest that the decay proceeds mostly through $K_1(1400)$. The latest measurements by CLEO [3] and ALEPH [1,2] as well as this analysis suggest $K_1(1270)$ dominance.

Combining our value of α with the known K_1 decay branching fractions, one can determine the $\overline{K}^{*0}\pi^-$ and $K^-\rho^0$ fractions in $\tau^- \to K^-\pi^+\pi^-\nu_\tau$ decays as

$$\frac{K^-\rho^0}{\overline{K}^{*0}\pi^-} = \frac{B_1 + B_2}{B_3 + B_4} = 0.82 \pm 0.37,$$

where

$$B_1 = \mathcal{B}(\tau^- \to K_1(1270)^-\nu_\tau) \cdot \mathcal{B}(K_1(1270)^- \to K^-\rho^0) \cdot \mathcal{B}(K^-\rho^0 \to K^-\pi^+\pi^-)$$

$$B_2 = \mathcal{B}(\tau^- \to K_1(1400)^-\nu_\tau) \cdot \mathcal{B}(K_1(1400)^- \to K^-\rho^0) \cdot \mathcal{B}(K^-\rho^0 \to K^-\pi^+\pi^-)$$

$$B_3 = \mathcal{B}(\tau^- \to K_1(1270)^-\nu_\tau) \cdot \mathcal{B}(K_1(1270)^- \to \overline{K}^{*0}\pi^-) \cdot \mathcal{B}(\overline{K}^{*0}\pi \to K^-\pi^+\pi^-)$$

$$B_4 = \mathcal{B}(\tau^- \to K_1(1400)^-\nu_\tau) \cdot \mathcal{B}(K_1(1400)^- \to \overline{K}^{*0}\pi^-) \cdot \mathcal{B}(\overline{K}^{*0}\pi \to K^-\pi^+\pi^-)$$

This corresponds to $K^-\rho^0/K^-\pi^+\pi^- = (45 \pm 11)\%$. This result is close to the measurement by ALEPH [2] $(35 \pm 11)\%$ of the same quantity, although no interference effects were taken into account in that measurement. This number also agrees with the measurement by ALEPH of another related decay channel, $\tau^- \to K^0_S\pi^-\pi^0\nu_\tau$ where the component $\overline{K}^0\rho^-$ in the intermediate state is found to be $(64 \pm 9 \pm 10)\%$, approximately twice larger due to isospin symmetries [1].

B. K_1 width

The question of the K_1 widths is of special interest because the theoretical predictions from models based on CHPT [8] provide predictions for branching fractions that are significantly higher [8] than current experimental values [2,12]. This discrepancy can be resolved if the K_1 resonances in τ decays are much wider than presently tabulated values. In the non-strange sector, it has long been realized that the a_1 width is considerably larger as measured in $\tau^- \to a_1^-\nu_\tau$ compared to hadronic production of the a_1.

It is possible from our fit to obtain information on the widths of the $K_1(1270)$ and $K_1(1400)$. The sensitivity to these widths is, however, limited due to the high degree of correlation between the fit parameters. In particular, the relative fractions of K_1 resonances (α) depends upon the widths. It is important to realize that if the widths of the K_1's in tau decays are much different than the current Particle Data Group values, our extraction of α, and its associated error, must be re-evaluated. Such an analysis, in which the K_1 widths are now included as a fit parameter, is currently underway.

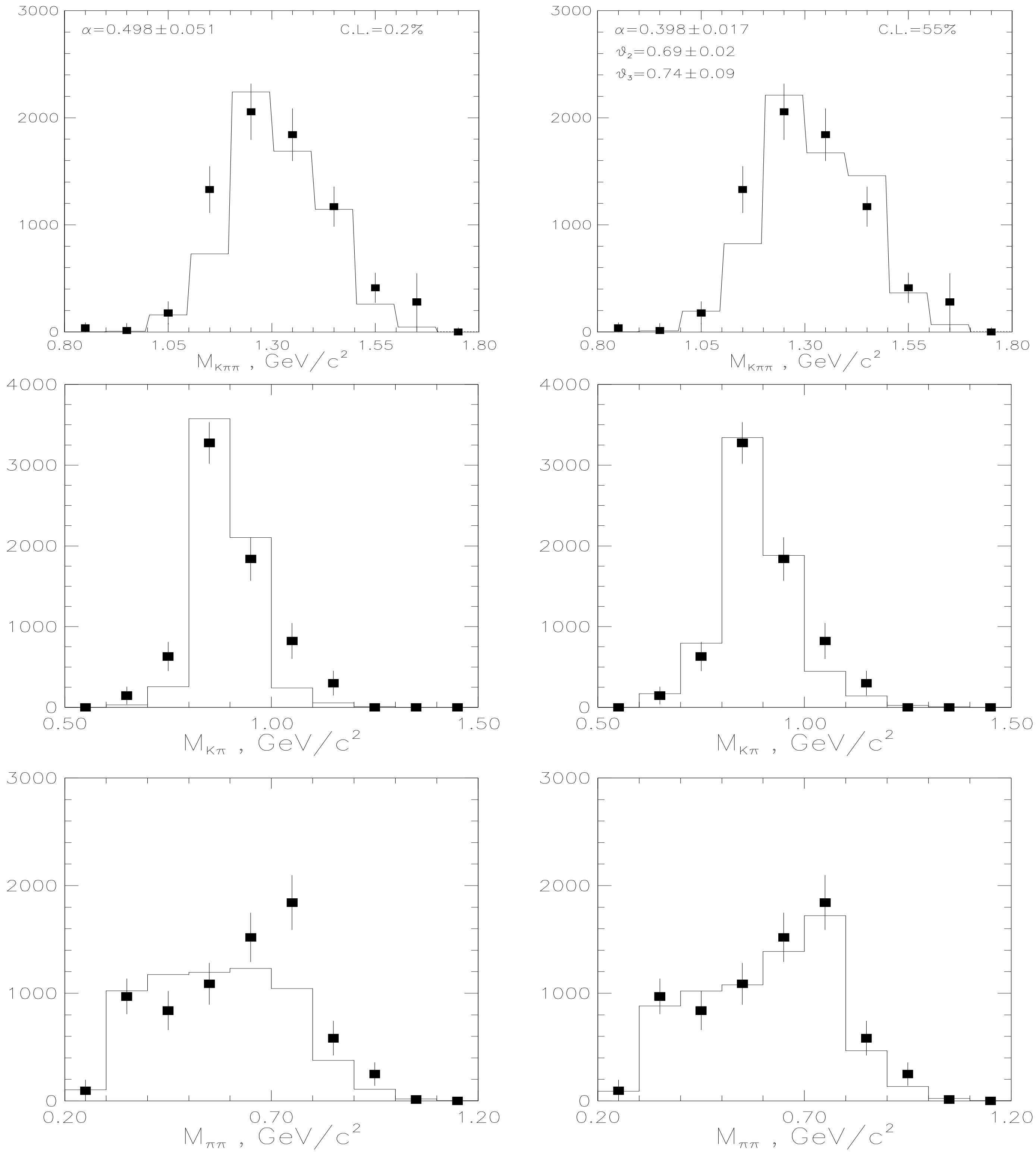

FIG. 2. Left-hand column of plots correspond to the simultaneous fit of data with free parameter α only, right-hand column is the fit of data with free parameters (α, θ_2, θ_3).

TABLE I. Summary of systematic errors. (Errors on θ_2 and θ_3 are given as fractions of 2π).

Source	Corresponding systematic errors		
	α, %	θ_2	θ_3
K_1 mean and width	14	0.02	0.04
K_1 branching fractions	7	0.03	0.06
Model dependence	14	0.03	0.07
Background	4	0.02	0.06
Fitting method	1	< 0.01	0.01
Total	22	0.05	0.12

VIII. SYSTEMATIC UNCERTAINTIES

Systematic errors are summarized in Table I. The dominant errors are due to the uncertainty in the K_1 mass, width and branching fractions, and the uncertainty in the background. The first error is estimated by varying the K_1 resonance parameters $\pm 1\sigma$ from the presently tabulated values [15] and repeating the data fits. The errors associated with the uncertainty in the branching fractions of the K_1's to $K^*\pi$ and $K\rho$ are estimated by changing the values for these branching fractions in the form-factors F_1 and F_2 within one standard deviation of the PDG values [15]. The resulting spread in the fit values is taken as the corresponding systematic error.

The uncertainty in the background is large because of the uncertainty in the branching fraction of its largest component, $\tau^- \to K^-K^+\pi^-\nu_\tau$. During the background subtraction the level of all τ-related backgrounds are varied by amounts corresponding to the errors on the branching fractions of these decays [12,15]. The hadronic background is similarly varied by 100% to determine the systematic error due to our uncertainty in the $q\bar{q}$ contribution to our candidate signal event sample.

Another large error comes from the choice of models in our Monte Carlo simulation. This includes the uncertainty in the shape of the kaon momentum spectrum used to obtain the total number of events with kaons [12], and the uncertainty in the shape of the invariant mass distribution for the $\tau^- \to K^-K^+\pi^-\nu_\tau$ background. These errors are estimated by using several different models to extract the invariant mass spectra, namely $\tau^- \to K_1(1270)^-\nu_\tau$ and $\tau^- \to K_1(1400)^-\nu_\tau$ with $0 < \alpha < 1$ for $\tau^- \to K^-\pi^+\pi^-\nu_\tau$ and the model described in [9], and $\tau^- \to a_1^-\nu_\tau \to K^{*0}K^-\nu_\tau$, $\tau^- \to \rho(1690)^-\nu_\tau \to K^{*0}K^-\nu_\tau$ and the model described in [9] for $\tau^- \to K^-K^+\pi^-\nu_\tau$.

There are three primary fitting function uncertainties. The first is the contribution from the ρ' which may be different in this decay from that observed in $e^+e^- \to \pi^+\pi^-$ data [10] due to the phase space suppression of ρ' in our case. Second, the model implemented in the fitting function contains no Wess-Zumino term. The corresponding fitting function errors from these two sources are estimated by varying the level of the Wess-Zumino term and the ρ' amplitudes from zero to the prediction of [8]. Finally, there is an uncertainty in the phase angle θ_1. The error due to this uncertainty is calculated by varying θ_1 over the interval $0-2\pi$ and refitting the data. Because the fitting function is based upon Monte Carlo, the Monte Carlo statistical error is also included here.

The systematics associated with the fitting of the invariant mass distribution ("Fitting method" in Table I) is studied using 60 samples of signal Monte Carlo with a full detector simulation. The results of this study shows no systematic shift of the fitted parameter values relative to the input values; the spread is fully consistent with that expected from statistics.

Because in this analysis only the shape of the invariant mass distribution is of interest, possible systematic effects that affect the overall normalization of the reconstructed spectra are ignored. Among such effects are trigger and tracking efficiencies, the photon veto, dE/dx extraction systematics and small non-τ backgrounds (2-photon events, beam-gas interactions, QED background).

IX. SUMMARY AND CONCLUSIONS

In this analysis we have measured the relative fractions and interference effects between the K_1 resonances in $\tau^- \to K^-\pi^+\pi^-\nu_\tau$ decays. These measurements are made within the framework of the model described in Sec. VI. The parameters of the K_1 resonances such as masses, widths and branching fractions have been set in this analysis to the values tabulated in [15]. Our parameterization of the axial vector form factors is different from [8] in two respects, as described in Sec. VI. First, we use isospin relations to determine the relative strength of different terms in the form-factors rather than the CHPT predictions in the chiral limit. Second, our data suggest the existence of phase shifts between the terms in the form-factors. Three phase angles θ_1, θ_2 and θ_3 are introduced; of these, our fit is sensitive to θ_2 and θ_3 which correspond to interference between $K_1(1270) \to K^*\pi \to K\pi\pi/K_1(1400) \to K^*\pi \to K\pi\pi$ and $K^*\pi \to K\pi\pi/K\rho \to K\pi\pi$, respectively. We find:

$$\alpha = 0.398 \pm 0.016 \pm 0.088$$

$$\theta_2 = (0.69 \pm 0.02 \pm 0.05) \cdot 2\pi$$

$$\theta_3 = (0.74 \pm 0.09 \pm 0.12) \cdot 2\pi$$

These measurements agree well with the recent results from CLEO and ALEPH (see Sec VII A). Finally, our data favor $K_1(1270)$ dominance in production of the $K^-\pi^+\pi^-$ final state.

ACKNOWLEDGMENTS

We gratefully acknowledge the effort of the CESR staff in providing us with excellent luminosity and running conditions. J.R. Patterson and I.P.J. Shipsey thank the NYI program of the NSF, M. Selen thanks the PFF program of the NSF, M. Selen and H. Yamamoto thank the OJI program of DOE, J.R. Patterson, K. Honscheid, M. Selen and V. Sharma thank the A.P. Sloan Foundation, M. Selen and V. Sharma thank Research Corporation, S. von Dombrowski thanks the Swiss National Science Foundation, and H. Schwarthoff thanks the Alexander von Humboldt Stiftung for support. This work was supported by the National Science Foundation, the U.S. Department of Energy, and the Natural Sciences and Engineering Research Council of Canada.

REFERENCES

[1] ALEPH Collaboration, R. Barate *et al.*, CERN-PPE/97-167 (1997).
[2] ALEPH Collaboration, R. Barate *et al.*, CERN-PPE/97-69, (1997).
[3] CLEO Collaboration, T. Coan *et al.*, Phys. Rev. **D53**, 6037 (1996).
[4] S. Towers, Nuclear Physics B (Proc. Suppl.) **55C**, 137, 1997; (Proceedings of *TAU96: Fourth Workshop on Tau Lepton Physics*, Estes Park, Colorado, September 16-19, 1996, ed. J.G. Smith and W. Toki).
[5] M. Suzuki, Phys. Rev. **D47**, 1252 (1993).
[6] A. Weinstein and R. Stroynowski, Ann. Rev. Nucl. Part. Sci 43, 457 (1993).
[7] R. Decker, E. Mirkes, R. Sauer, and Z. Was, Z. Phys. **C58**, 445 (1993).
[8] M. Finkemeier and E. Mirkes, Z. Phys. **C69**, 243 (1996).
[9] S. Jadach, Z.Was, R. Decker and J. H. Kühn, CERN-TH.6793/93.
[10] J. H. Kühn and A. Santamaria, Z. Phys. C48 , 445 (1990).
[11] CLEO Collaboration, Y. Kubota *et al.*, Nucl. Inst. Meth. **320** 66, (1992).
[12] CLEO Collaboration, S. J. Richichi *et al.*, Report No. CLNS 98/1573 (to be published).
[13] JETSET 7.3: T. Sjöstrand and M. Bengtsson, Comput. Phys. Commun. **43**, 367 (1987).
[14] R. Brun *et al.*, "GEANT3 Users Guide," CERN DD/EE/84-1 (1987).
[15] R. M. Barnett *et al.*, Phys. Rev. **D54**, 1 (1996).
[16] D. A. Bauer, Phys. Rev. **D50**, R13 (1994).

APPENDIX A: ISOSPIN COEFFICIENTS FOR AXIAL VECTOR FORM-FACTORS

The relative strength of the form-factors F_1 and F_2 can be determined from the isospin relations relevant for the processes (A1)-(A4).

$$\tau^- \to K_1(1270)^- \nu_\tau \to K^- \rho^0 \nu_\tau \to K^- \pi^+ \pi^- \nu_\tau \tag{A1}$$

$$\tau^- \to K_1(1400)^- \nu_\tau \to K^- \rho^0 \nu_\tau \to K^- \pi^+ \pi^- \nu_\tau \tag{A2}$$

$$\tau^- \to K_1(1270)^- \nu_\tau \to \overline{K}^{*0} \pi^- \nu_\tau \to K^- \pi^+ \pi^- \nu_\tau \tag{A3}$$

$$\tau^- \to K_1(1400)^- \nu_\tau \to \overline{K}^{*0} \pi^- \nu_\tau \to K^- \pi^+ \pi^- \nu_\tau \tag{A4}$$

The K_1 particle can be represented as $|I, I_Z\rangle = |\frac{1}{2}, -\frac{1}{2}\rangle$. Here (and later), the notation K_1 implies either $K_1(1270)$ or $K_1(1400)$. In the decay of K_1 to $K\rho$ we have two possible charge combinations: $|\rho^0 K^-\rangle$ and $|\rho^- \overline{K}^0\rangle$. Using the table of Clebsch-Gordan coefficients [15], we obtain:

$$|\frac{1}{2}, -\frac{1}{2}\rangle \to \frac{1}{\sqrt{3}}|0, -\frac{1}{2}\rangle - \sqrt{\frac{2}{3}}|-1, \frac{1}{2}\rangle, \tag{A5}$$

where on the right-hand side the isospin projections of the decay products are given: $|I_{1z}, I_{2z}\rangle$. Because $\rho^- \to \pi^-\pi^0$ only and $\rho^0 \to \pi^+\pi^-$ only,

$$K_1 \to \frac{1}{\sqrt{3}}|(\pi^-\pi^+)K^-\rangle - \sqrt{\frac{2}{3}}|(\pi^-\pi^0)\overline{K}^0\rangle \tag{A6}$$

Analogous calculations can be done for $K_1 \to K^*\pi$. There are two possible alternate decay routes: $K^{*-}\pi^0$ and $\overline{K}^{*0}\pi^-$. The isospin equation (A5) holds true for these two decays as well. For these decays we write:

$$K_1 \to \frac{1}{\sqrt{3}}|\pi^0 K^{*-}\rangle - \sqrt{\frac{2}{3}}|\pi^-\overline{K}^{*0}\rangle$$

For K^{*-} the isospin equation is the same as Eq.(A5):

$$K^{*-} \to \frac{1}{\sqrt{3}}|\pi^0 K^-\rangle - \sqrt{\frac{2}{3}}|\pi^-\overline{K}^0\rangle$$

For $\overline{K}^{*0}$ decays, the isospin relation is different:

$$|\frac{1}{2}, \frac{1}{2}\rangle \to \sqrt{\frac{2}{3}}|1, -\frac{1}{2}\rangle - \frac{1}{\sqrt{3}}|0, \frac{1}{2}\rangle$$

corresponding to:

$$\overline{K}^{*0} \to \sqrt{\frac{2}{3}}|\pi^+, K^-\rangle - \frac{1}{\sqrt{3}}|\pi^0, \overline{K}^0\rangle$$

Adding the two possible paths for $K_1 \to K^*\pi$, we obtain:

$$K_1 \to \frac{1}{3}|\pi^0(\pi^0 K^-)\rangle - \frac{\sqrt{2}}{3}|\pi^0(\pi^-\overline{K}^0)\rangle - \frac{2}{3}|\pi^-(\pi^+K^-)\rangle + \frac{\sqrt{2}}{3}|\pi^-(\pi^0\overline{K}^0)\rangle \tag{A7}$$

Given that our final state is $K^-\pi^+\pi^-$, from the expressions (A6) and (A7) it follows that the form-factors F_1 and F_2 should be added with coefficients $\frac{1}{\sqrt{3}}$ and $-\frac{2}{3}$, respectively.